Extended state observer-based robust pitch autopilot design for tactical missiles

A A Godbole, T R Libin, and **S E Talole***
Department of Aerospace Engineering, Defence Institute of Advanced Technology, Girinagar, India

The manuscript was received on 9 May 2011 and was accepted after revision for publication on 21 September 2011.

DOI: 10.1177/0954410011426397

Abstract: In this article, a new design based on the extended state observer (ESO) technique for the pitch autopilot of a tail-controlled, skid-to-turn missile is proposed. The pitch-plane dynamics with the angle of attack as output is significantly uncertain. The ESO simultaneously estimates the state and the uncertainty. The estimated uncertainty is used to robustify the input–output–linearization-based controller designed for the nominal system. Closed-loop stability of the observer–controller combination is proved. The notable feature of the proposed design is that it neither requires accurate plant model nor any information about the uncertainty. The effectiveness of the ESO in estimation of the uncertainties and states and in meeting the specified tracking performance in the presence of significant uncertainties is illustrated by simulation. Finally, to demonstrate the efficacy of the proposed design, comparison of its performance with some of the well-known existing controllers is presented.

Keywords: pitch autopilot, input–output linearization, extended state observer, robust control

1 INTRODUCTION

Missile autopilots are traditionally designed using classical linear control approaches. In general, the missile dynamics is linearized around certain finite number of operating points in the flight envelope, and linear controllers designed at these points are then gain-scheduled to obtain desired performance in the complete flight envelope. To this end, the linear control techniques have dominated missile autopilot design over the past several decades [**1**, **2**]. As robustness is a matter of great concern, various robust control techniques such as H_∞ and μ analysis [**3**–**5**] have been proposed to design robust autopilots. One can also find specific theories such as control of linear parametrically varying systems [**6**, **7**], eigenstructure assignment technique [**8**], and extended-mean assignment technique for linear time-varying systems [**9**] employed for the design of missile autopilot.

Although design of autopilots following linearization and gain scheduling is one of the most prominent approach, the controller thus designed may offer unsatisfactory performance, especially when the dynamics is highly non-linear and undergoes large motion. The ever increasing high performance and greater manoeuvrability requirements now demand the missiles to operate in regimes of large angles and angular rates where non-linearities are dominant. For example, the missiles having wingless configurations will need to execute high-angle of attack manoeuvres to generate the desired acceleration levels. As it is well known, the aerodynamics at high angle of attack are difficult to model accurately, giving rise to not having accurate mathematical model for control design. In these circumstances, the performance of traditional linear control techniques may not be satisfactory. Another disadvantage of gain-scheduled controller is the complexity involved in gain interpolation of the controllers. These issues have motivated the use of non-linear approaches for designing missile autopilots and to this end, one can find applications of

*Corresponding author: *Department of Aerospace Engineering, Defence Institute of Advanced Technology, Girinagar, Pune 411 025, India.*
email: setalole@hotmail.com

various non-linear control theories for autopilot design. Controllers based on non-linear predictive control [**10**], sliding mode control (SMC) [**11**], and adaptive back-stepping [**12**] are some examples to cite.

The input–output linearization (IOL) [**13**, **14**] is one prominent approach in non-linear control systems design. One of the advantages offered by IOL is that it provides a systematic framework for designing controllers for non-linear systems. The dynamic inversion approach in aerospace literature and inverse dynamics technique in robotics are essentially input-output linearizing controllers. However, as it is well known, the IOL theory is not directly applicable for designing acceleration-tracking controllers in tail-controlled missiles due to the non-minimum phase characteristics of the acceleration dynamics. To overcome this issue, controllers have been frequently designed through output redefinition, i.e. using angle of attack (or combination of angle of attack and pitch rate) as output instead of the normal acceleration [**9**, **10**, **12**, **15**–**17**]. To cite some more examples, an augmented acceleration signal that is dependent on lateral velocity is used for tracking purpose in references [**18**–**20**]. In reference [**21**], a dynamic inversion-based inner-loop control is used with angle of attack as output. Similarly, a gain-scheduled missile autopilot design is presented in reference [**7**], wherein the inner loop consists of an angle of attack servo design. In such designs, usually, the desired acceleration command is translated into an equivalent angle of attack command and the controller is asked to track the latter.

There exist certain issues in IOL-based control design that need attention. The IOL-based controller offers satisfactory performance only when the model is known exactly. In reality, it is difficult to meet this condition and so the IOL control laws may not offer satisfactory performance. One approach to address the issue of degradation in performance of the IOL controller in the presence of uncertainties is to robustify it and to this end, various approaches have been proposed in the literature. For example, the problem of stabilization of a class of non-linear systems with time-varying uncertain parameters is presented by Chen and Chen [**22**], wherein a Lyapunov function-based robust controller is incorporated with feedback linearization to guarantee the practical stability. A robust outer loop design based on the Lyapunov's second method is presented in reference [**23**] for the design of an autopilot of a BTT missile. An angle of attack tracking controller based on IOL is presented in reference [**15**], wherein to achieve robustness, the controller is augmented by adding a term which is based on the assumed bound of uncertainty. Robust feedback linearization has also been approached by the sliding mode control (SMC) technique [**24**, **25**] in the literature. In all these approaches, the uncertainties are assumed to be norm-bounded and thus it becomes necessary to have the knowledge of the bounds. While the use of highly conservative bound results in excessive control effort, use of lower bounds may result in degradation of performance or even in instability. Another important issue in IOL controller is the requirement of state vector and output derivatives for feedback. If the required states and derivatives are not measured/available, the same are required to be estimated necessitating a separate design for an observer.

In this article, design of a pitch autopilot for a tail-controlled, roll position-stabilized, skid-to-turn missile that is implementable and robust to uncertainties, modelling inaccuracies, and external disturbances is proposed. In this design, an extended state observer (ESO) is employed to obtain the estimate of the composite uncertainty as well as the system states in an integrated manner. Application of ESO in designing a robust roll autopilot is presented in reference [**26**], wherein LQR-based roll controller existing in literature is robustified by augmenting the same with the ESO estimated uncertainties and it is shown that the resulting controller offers better robustness in the face of parametric uncertainties, external disturbances, airframe flexibility, and fast un-modeled sensor lags in comparison with the existing design. This study deals with design of pitch autopilot using the ESO. Here, an IOL controller is designed for angle of attack tracking and in doing so, the effects of discrepancies associated with various aerodynamic derivatives, modelling errors, and external disturbances are treated as a composite uncertainty required to be estimated. As the IOL control needs estimation of the first and second derivatives of the angle of attack, an ESO is designed to estimate the composite uncertainty as well as the output derivatives in an integrated manner. The design neither needs exact system model nor a knowledge of any characteristic of the uncertainty. Closed-loop stability of the system under the proposed controller is established. Simulations are carried out by considering significant uncertainties in aerodynamic parameters, un-modelled dynamics, and control input and rate saturation to demonstrate the effectiveness of the approach in realistic scenario and the results presented. Finally, the performance of the proposed controller is compared with some well-known existing non-linear designs to demonstrate the efficacy of the proposed approach.

The remaining article is organized as follows: section 2 presents the non-linear missile dynamics and controller design based on the IOL approach. In

section 3, the theory of ESO is briefly reviewed and applied for the state and uncertainty estimation of the present problem. Closed-loop stability results are presented in section 4, while simulation results demonstrating the effectiveness of the proposed design are given in section 5. Comparison results of the proposed controller with some well-known existing designs are presented in section 6 and finally, section 7 concludes this study.

2 IOL-BASED CONTROL

This study deals with the design of a pitch autopilot for a tail-controlled, roll position-stabilized, skid-to-turn tactical missile, wherein the objective is to force the missile to track a desired or commanded angle of attack. In what follows is the mathematical model used in the design and formulation of the IOL-based controller.

2.1 Non-linear missile model

The mathematical model of a missile used here describes the non-linear pitch-axis dynamics of a highly manoeuvrable air-to-air missile [**3**]. The model is well known and has been used in a number of studies in the literature [**5**, **6**, **8**] for design and analysis of pitch plane controllers. The equations that govern the missile dynamics, including a first-order servo are given as

$$\begin{aligned}\dot{\alpha}(t) &= K_\alpha M(t) C_n[\alpha(t), \delta(t), M(t)] cos(\alpha(t)) + q(t)\\ \dot{q}(t) &= K_q M^2(t) C_m[\alpha(t), \delta(t), M(t)]\\ \dot{\delta}(t) &= -\omega_a \delta(t) + \omega_a \delta_c(t)\end{aligned} \tag{1}$$

where α is the angle of attack (rad), q the pitch rate (rad/s), δ the control surface deflection (rad), M the Mach number, ω_a the actuator bandwidth, and δ_c the control input (rad). The aerodynamic force and moment coefficients, C_n and C_m, which reflect the aerodynamic non-linearity and parameter dependence are given by

$$\begin{aligned}C_n(\alpha,\delta,M) &= a_n\alpha^3 k^3 + b_n\alpha|\alpha|k^2 + c_n\left(2-\frac{M}{3}\right)\alpha k\\ &\quad + d_n k\delta\\ C_m(\alpha,\delta,M) &= a_m\alpha^3 k^3 + b_m\alpha|\alpha|k^2 + c_m\left(-7+\frac{8M}{3}\right)\alpha k\\ &\quad + d_m k\delta\end{aligned}$$

where $k = \left(\frac{180}{\pi}\right)$ is the radian-to-degree conversion factor. The data are valid for the operational range of $1.5 \leqslant M \leqslant 3$ and $-20^\circ \leqslant \alpha \leqslant +20^\circ$. The variation in missile velocity can be taken into account on using the Mach number dynamics given by

$$\dot{M}(t) = \frac{1}{v_s}[-|a_z(t)|\sin|\alpha(t)| + a_x M^2(t)\cos\alpha(t)] \tag{2}$$

where a_z and a_x are the normal and longitudinal accelerations, respectively, of the missile. The Mach number dynamics (2) can be used along with (1) in simulation to analyse the performance of the controller in realistic scenario. The details of the pitch axis missile model data and the constants are given in Table 1. The performance objectives for the proposed design are to force the missile to track a desired or commanded angle of attack with a time constant of less than 0.25 s with less than 10 per cent overshoot and less than 1 per cent steady-state error. The design is expected to offer robustness in the operational range $1.5 \leqslant M \leqslant 3$ and $-20^\circ \leqslant \alpha(t) \leqslant +20^\circ$ in the presence of C_n and C_m being uncertain by ± 25 per cent. The design is also expected to offer stability and desired performance throughout its operational flight envelope in the presence of unmodelled dynamics and actuator position and rate saturation.

2.2 IOL-based control

The basic idea underlying the I–O linearization is to obtain a non–linear controller which seeks to linearize the otherwise non–linear system. Once the system is linearized, any standard linear technique can be employed for designing the control law. To this end, the design consists typically of two steps; first, constructing a non-linear control law as an *inner loop control*, and then designing a second-stage or *outer loop control* to obtain the desired closed-loop performance. In this section, the IOL theory is used for designing an angle of attack-tracking controller.

Consider the missile dynamics given by (1). It can be noticed that with angle of attack, α, as output and commanded fin deflection, δ_c, as input, the

Table 1 Details of pitch axis missile model

P_0 = static pressure at 6096 m	46 601.6 N/m^2
S = surface area	0.040 877 m^2
m = mass	204.01 kg
v_s = speed of sound	315.89 m/s
d_r = diameter	0.2286 m
I_y = pitch moment of inertia	247.42 kg m^2
C_a = drag coefficient	−0.3
$K_\alpha = (0.7)P_0S/mv_s$	
$K_q = (0.7)P_0Sd_r/I_y$	
$K_z = (0.7)P_0S/m$	
ω_a = actuator natural frequency	150 rad/s
ζ_a = actuator damping	0.7
$a_n = 0.000\,103$ deg^{-3}	$a_m = 0.000\,215$ deg^{-3}
$b_n = -0.009\,45$ deg^{-2}	$b_m = -0.0195$ deg^{-2}
$c_n = -0.169\,6$ deg^{-1}	$c_m = 0.051$ deg^{-1}
$d_n = -0.034$ deg^{-1}	$d_m = -0.206$ deg^{-1}

relative degree is 2. However, as it is well known, the control surfaces are primarily moment-producing devices and thus their contribution in the force equation can be ignored [**12**, **15**, **21**, **23**]. Ignoring the control surface deflection terms also leads to improved relative degree, as shown in reference [**19**]. For example, taking $d_n \approx 0$ in the aerodynamic coefficient, C_n, results into relative degree of 3 which is same as the order of the system. Thus zero dynamics will not be present in the resulting design. Also, in formulating the IOL control, $\cos(\alpha) \approx 1$ is taken since the error introduced due to this assumption is small in the specified range of angle of attack $-20^\circ \leqslant \alpha(t) \leqslant +20^\circ$ [**6**]. Following these assumptions, i.e. taking $d_n = 0$ and setting $\cos(\alpha) = 1$, and differentiating α three times, i.e. till the control input, δ_c, appears explicitly, yields

$$\begin{aligned}\dddot{\alpha} = {} & K_q M^2(3a_m k^3\alpha^2 + 2b_m k^2|\alpha| + c_m(-7+8M/3)k)\dot{\alpha} \\ & - K_q M^2 d_m k\omega_a\delta + K_\alpha M(6a_n k^3\alpha + 2b_n k^2 sgn(\alpha))\dot{\alpha}^2 \\ & + K_\alpha M(3a_n\alpha^2 k^3 + 2b_n|\alpha|k^2 + c_n(2-M/3)k)\ddot{\alpha} \\ & + K_q M^2 d_m k\omega_a\delta_c \end{aligned} \tag{3}$$

Re-writing (3) as

$$\dddot{\alpha} = a + b\delta_c \tag{4}$$

where the non-linear functions, a and b are defined as

$$\begin{aligned} a \triangleq {} & K_q M^2(3a_m k^3\alpha^2 + 2b_m k^2|\alpha| + c_m(-7+8M/3)k)\dot{\alpha} \\ & - K_q M^2 d_m k\omega_a\delta + K_\alpha M(6a_n k^3\alpha + 2b_n k^2 sgn(\alpha))\dot{\alpha}^2 \\ & + K_\alpha M(3a_n\alpha^2 k^3 + 2b_n|\alpha|k^2 + c_n(2-M/3)k)\ddot{\alpha} \\ b \triangleq {} & K_q M^2 d_m k\omega_a \end{aligned} \tag{5}$$

Using the IOL theory, the inner loop control is

$$\delta_c = \frac{1}{b}(-a+\nu) \tag{6}$$

where ν represents the outer loop control which is designed as

$$\nu = \dddot{\alpha}^\star + m_1(\alpha^\star - \alpha) + m_2(\dot{\alpha}^\star - \dot{\alpha}) + m_3(\ddot{\alpha}^\star - \ddot{\alpha}) \tag{7}$$

In (7), the starred quantities represent the reference values of the corresponding variables. Substituting (7) in (6) and applying the resulting control law to (4), results in output tracking error dynamics as

$$\frac{\mathrm{d}^3 e_{c_1}}{\mathrm{d}t^3} + m_3\frac{\mathrm{d}^2 e_{c_1}}{\mathrm{d}t^2} + m_2\frac{\mathrm{d}e_{c_1}}{\mathrm{d}t} + m_1 e_{c_1} = 0 \tag{8}$$

where $e_{c_1}(t) = \alpha^\star(t) - \alpha(t)$ is the output tracking error. The values of the gains, m_i, being design parameters, are required to be chosen such that closed-loop stability and desired tracking performance are achieved.

Now, some comments on the IOL controller presented in this section are in order. The controller (6) requires exact information of the system model, a condition which is hard to satisfy in practical scenario. Also, the controller needs output derivatives, i.e. $\dot{\alpha}$ and $\ddot{\alpha}$ for its implementation. In the present case, the angle of attack is assumed to be available and thus the estimation of its higher order derivatives becomes necessary. Finally, the controller performance will be affected whenever the system is subjected to external disturbances. The issues need to be addressed and in this study, the same has been done using an ESO, as discussed in the next section.

3 ESO-BASED CONTROL

As discussed in the last section, the IOL controller (6) lacks robustness. One strategy to robustify a given controller in the presence of uncertainties without requiring any knowledge of the same, is through uncertainty and disturbance estimation approach. The idea is to estimate the effect of uncertainties and disturbances and to use the opposite of it in the controller. To this end, a great deal of efforts have been devoted and a number of methods/approaches are proposed to robustify systems in the presence of the uncertainties and disturbances. To cite some examples, an application of the time delay control (TDC) to estimate the target acceleration, which is considered as a disturbance acting on the system, is presented in reference [**27**]. In reference [**28**], an IOL controller is robustified by estimating the uncertainties using uncertainty and disturbance estimation technique. As one more example, in reference [**29**], a sliding mode disturbance observer is designed to estimate the uncertainties/disturbances acting on the system. The estimated uncertainties are then used in the controller to compensate them. Applications of disturbance estimation and rejection can also be found in autopilot design problems. For example in reference [**30**], an observer is designed for roll channel to estimate the aerodynamic disturbance term. In reference [**17**], a neural network-based adaptive element is added to the dynamic inversion-based controller for the purpose of compensation of inversion errors. A design of a non-linear disturbance observer to robustify the pitch controller of a missile can be found in reference [**16**]. Similarly, in reference [**21**], a neural network is employed to robustify the inner loop dynamic inversion controller designed for pitch autopilot.

In the context of the present problem, while one can design disturbance observer/estimator to address the issue of robustness, a separate observer design would also be needed for estimating the output derivatives. In this circumstance, it is desirable to have the estimation of uncertainties as well as the output derivatives in an integrated manner and this requirement is met by the ESO.

3.1 Extended state observer

In the ESO formulation [**31**–**33**], the combined or total effect of uncertainties, non-linearities, modelling inaccuracies, and external disturbances acting on the system is treated as an extended state of the system. The ESO estimates the state of the extended order system, leading to estimation of the total uncertainty or disturbance along with the system states enabling disturbance rejection or compensation. Since the observer estimates the total uncertainty as an extended state of the system, it is known as ESO. Having estimated the states and the effect of uncertainties and disturbances, one can design a state feedback controller for nominal model of the system and augment it with the estimate of uncertainties to achieve robustness. While the vast majority of observer designs appeared in literature require accurate mathematical model of the system, the ESO is relatively independent of it, thus offering inherent robustness. Further, it is simple to implement. A comparison study of three advanced state observers, namely high-gain observer, ESO, and sliding-mode observer is presented in reference [**31**] and the authors have shown that overall the ESO offers superior performance in dealing with the uncertainties, disturbances, and sensor noise. A large number of diverse applications of ESO-based control strategies have been reported in literature. ESO is in various applications such as disturbance rejection control for uncertain multi-variable systems with time delay [**34**], control of flexible joint system [**35**], aircraft attitude control [**36**], robust roll autopilot design for tactical missiles [**26**], attitude tracking of rigid spacecraft [**37**], and torsional vibration control [**38**]. In this section, a brief review of this approach [**31**–**33**, **39**–**42**] is presented for the sake of ready reference and the reader may refer to the various references cited above for more details.

Consider an nth order, single-input–single-output non-linear dynamical system described by

$$\overset{(n)}{y} = a\left(y, \dot{y}, \ldots, \overset{(n-1)}{y}\right) + bu + w \tag{9}$$

where $a(\cdot)$ represents the dynamics of the plant, $w(t)$ an unknown disturbance, $u(t)$ the control input, and $y(t)$ the measured output. Let $a(\cdot) = a_o(\cdot) + \Delta a(\cdot)$, where $a_o(\cdot)$ is either the best available estimate of $a(\cdot)$ or a known part of it and $\Delta a(\cdot)$ the uncertainty associated with it. Similarly, let $b = b'_o + \Delta b$, where b'_o is the best available estimate of b, while Δb is its associated uncertainty. If the knowledge of $a_o(\cdot)$ is not available, the complete quantity, i.e. $a(\cdot)$ may be treated as unknown and would form a part of the uncertainty required to be estimated [**31**]. Now, defining the total uncertainty as $d \triangleq \Delta a + \Delta b u + w$ and designating it as an extended state, x_{n+1}, the dynamics of (9) is re-written in a state-space form as

$$\begin{aligned}
\dot{x}_1 &= x_2 \\
\dot{x}_2 &= x_3 \\
&\vdots \\
\dot{x}_n &= x_{n+1} + a_o + b'_o u \\
\dot{x}_{n+1} &= h \\
y &= x_1
\end{aligned} \tag{10}$$

where h is the rate of change of the uncertainty, i.e. $h = \dot{d}$ and assumed to be an unknown but bounded function. By making, d, a state, however, it is now possible to estimate it using a state estimator. To this end, consider a non-linear observer of the form

$$\begin{aligned}
\dot{\hat{x}}_1 &= \hat{x}_2 + \beta_1 g_1(e_{o_1}) \\
\dot{\hat{x}}_2 &= \hat{x}_3 + \beta_2 g_2(e_{o_1}) \\
&\vdots \\
\dot{\hat{x}}_n &= \hat{x}_{n+1} + \beta_n g_n(e_{o_1}) + a_o + b'_o u \\
\dot{\hat{x}}_{n+1} &= \beta_{n+1} g_{n+1}(e_{o_1})
\end{aligned} \tag{11}$$

where $e_{o_1} = y - \hat{y} = x_1 - \hat{x}_1$ and $\hat{x}_{n+1}$ is an estimate of the uncertainty, d. The quantities β_i are the observer linear gains, while $g_i(\cdot)$ are the set of suitably constructed non-linear gain functions satisfying $e_{o_1} g_i(e_{o_1}) > 0$, $\forall e_{o_1} \neq 0$ and $g_i(0) = 0$ [**41**, **42**]. If the non-linear functions, $g_i(\cdot)$ and their related parameters are chosen properly, the estimated states $\hat{x}_i$ are expected to converge to the respective states of the system x_i, i.e. $\hat{x}_i \to x_i$; $\quad i = 1, 2, \ldots, n+1$.

The choice of the non-linear gain function is an important aspect in the ESO design. The general expression for these functions, selected based on experimental results [**38**] is

$$\begin{aligned}
g_i(e_{o_1}, \mu_i, \epsilon) &= \begin{cases} |e_{o_1}|^{\mu_i} \operatorname{sign}(e_{o_1}), & |e_{o_1}| > \epsilon \\ \frac{e_{o_1}}{\epsilon^{1-\mu_i}}, & |e_{o_1}| \leqslant \epsilon \end{cases} \\
& i = 1, 2, \ldots, n+1
\end{aligned} \tag{12}$$

where $\varepsilon > 0$. It can be seen that with $\mu_i = 1$, $i = 1, \ldots, n+1$; $g_i(e_{o_1}) = e_{o_1}$ and the observer of (11) reduces to the classical Luenberger observer, while with $\mu_i = 0$, $i = 1, \ldots, n+1$; $g_i(e_{o_1})$ contains signum term and thus the resulting observer resembles the sliding-mode observer. It can also be seen that for $0 < \mu_i < 1$, $g_i(\cdot)$ yields relatively high gain when the error is small and small gain when the error is large. The quantity, ϵ, is a small number used to limit the gain in the neighbourhood of the origin and defines the range of the error corresponding to high gain [**31**]. It may be noted that the linear region in the neighbourhood of origin

prevents high-frequency chattering caused by the signum term. Usually, the ESO design proceeds with first selecting the linear gains, β_i's by assuming $g_i(e_{o_1}) = e_{o_1}$ and subsequently non-linear gain functions are designed to achieve better performance.

3.2 ESO-based controller

Now, rewriting the dynamics of (4) in the same form of (9) as

$$\ddot{\alpha} = a + b\delta_c + w \tag{13}$$

where a and b are as given in (5) and w represents an unknown external disturbance acting on the missile. Now, expressing the function a as

$$a = a_1\alpha + a_2\dot{\alpha} + a_3\ddot{\alpha} + d' \tag{14}$$

where $a_1 = 0$, $a_2 = K_q M^2 c_m(-7 + 8M/3)k$, $a_3 = K_\alpha M c_n(2 - M/3)k$ and d' represents the remaining terms. In view of (14), the angle of attack dynamics (13) takes the form

$$\ddot{\alpha} = a_1\alpha + a_2\dot{\alpha} + a_3\ddot{\alpha} + d' + w + bu \tag{15}$$

In the presence of the uncertainties in the aerodynamic derivatives and other parameters, the terms a_i's and b will not be known precisely. To account for it, the uncertainties are modelled as $a_i = a_{io} + \Delta a_i$ and $b = b_o + \Delta b$, where the a_{io}, b_o are the nominal values of the respective parameters and Δa_i, Δb their associated uncertainties. The total uncertainty that needs to be estimated is defined as

$$d = \Delta a_1\alpha + \Delta a_2\dot{\alpha} + \Delta a_3\ddot{\alpha} + \Delta b u + d' + w \tag{16}$$

Note that in defining the uncertainty in this manner, part of the dynamics, i.e. d' is also assumed as unknown. Apart from it, the uncertainty, d, may also include any other unknown factors such as the cross-coupling effects, effects of linearizing approximations, un-modelled dynamics, and also the effect of neglecting the contribution of control surface deflection in force equation. In view of the description of the uncertainty, the dynamics of (15) can be written as

$$\ddot{\alpha} = a_{1o}\alpha + a_{2o}\dot{\alpha} + a_{3o}\ddot{\alpha} + b_o u + d \tag{17}$$

and the resulting IOL controller becomes

$$u = \frac{1}{b_o}\Big[- a_{1o}\alpha - a_{2o}\dot{\alpha} - a_{3o}\ddot{\alpha} - d + \dddot{\alpha}^\star + m_1(\alpha^\star - \alpha) + m_2(\dot{\alpha}^\star - \dot{\alpha}) + m_3(\ddot{\alpha}^\star - \ddot{\alpha})\Big] \tag{18}$$

Applying the control law (18) to the dynamics of (17) results into the same tracking error dynamics, as given by (8). The controller (18) is designated as the IOL controller. From (18), it is obvious that to make the control law implementable, the estimate of the uncertainty, d, is required apart from the output derivatives and for this purpose, an ESO is designed as follows:

To facilitate ESO design, the dynamics (17) is rewritten in a phase-variable state space model as

$$\begin{aligned} \dot{x}_1 &= x_2 \\ \dot{x}_2 &= x_3 \\ \dot{x}_3 &= a_{1o}x_1 + a_{2o}x_2 + a_{3o}x_3 + b_o u + d \\ y &= x_1 \end{aligned} \tag{19}$$

where $x_1 = \alpha$, $x_2 = \dot{\alpha}$, and $x_3 = \ddot{\alpha}$ are the states; $y = \alpha$ the output, and $u = \delta_c$ the input. Defining $x_4 = d$, the extended order system takes the form as

$$\begin{aligned} \dot{x}_1 &= x_2 \\ \dot{x}_2 &= x_3 \\ \dot{x}_3 &= x_4 + a_{1o}x_1 + a_{2o}x_2 + a_{3o}x_3 + b_o u \\ \dot{x}_4 &= h \\ y &= x_1 \end{aligned} \tag{20}$$

where h is the rate of change of uncertainty. Writing (20) in compact state space notation as

$$\begin{aligned} \dot{x} &= Ax + Bu + Eh \\ y &= Cx \end{aligned} \tag{21}$$

where $x = [x_1\ x_2\ x_3\ x_4]^T$ is the state vector of the extended order system and

$$A = \begin{bmatrix} 0 & 1 & 0 & 0 \\ 0 & 0 & 1 & 0 \\ a_{1o} & a_{2o} & a_{3o} & 1 \\ 0 & 0 & 0 & 0 \end{bmatrix};\ B = \begin{bmatrix} 0 \\ 0 \\ b_o \\ 0 \end{bmatrix}$$

$$E = \begin{bmatrix} 0 \\ 0 \\ 0 \\ 1 \end{bmatrix};\ \text{and}\ C = [1\ 0\ 0\ 0]$$

The ESO of (11) with the gains, as given in (12), is referred to as the non-linear ESO or NESO since it employs the non-linear gain functions. If one chooses $g_i(e_{o_1}) = e_{o_1}$, the ESO takes the form of the well-known Luenberger observer and is designated as the LESO. Thus, the LESO essentially represents a special case of the non-linear ESO when the NESO parameters, μ_is, are chosen as unity. In this study, an LESO is employed instead of the NESO owing to certain advantages offered by it. First, in LESO, the observer gains can be chosen systematically through pole placement, whereas there does not exists a systematic procedure for selecting the various parameters in NESO. Second, the closed-loop stability analysis for LESO is straightforward, as shown in section 6.

Finally, the LESO is easy from hardware implementation point of view [**35**].

To this end, following the procedure outlined in earlier section, an ESO of the form of equation (11) with $g(e_{o_1}) = e_{o_1}$, $n = 3$, $b'_o = b_o$ is designed for the dynamics of equation (20) by taking the total uncertainty as an extended state, x_4 and is given by

$$\dot{\hat{x}} = A\hat{x} + Bu + L(y - \hat{y}) \tag{22}$$

where

$$L = [\beta_1 \ \beta_2 \ \beta_3 \ \beta_4]^T \tag{23}$$

is the observer gain vector. Having the estimates of states, the IOL controller (18) takes the following form

$$u = \frac{1}{b_o}[-a_{1o}\hat{x}_1 - a_{2o}\hat{x}_2 - a_{3o}\hat{x}_3 - \hat{x}_4 + \dot{x}_3^\star + m_1(x_1^\star - \hat{x}_1) + m_2(x_2^\star - \hat{x}_2) + m_3(x_3^\star - \hat{x}_3)] \tag{24}$$

where $\hat{x}_4$ is an estimate of the uncertainty, d. The controller (24) is designated as the ESO-based controller and is implementable. A notable feature of the design is that while it offers robustness, it needs only one measurement, i.e. angle of attack. A functional block diagram of the ESO-based controller is shown in Fig. 1.

4 CLOSED-LOOP STABILITY

In this section, closed-loop stability of the system given by equation (19) under the controller–observer structure is established, wherein the controller is given by (24) and the observer by (22). To this end, rewriting the pitch dynamics of (19) as

$$\dot{x}_p = A_p x_p + B_p u + B_d d \tag{25}$$

where $x_p = [x_1 \ x_2 \ x_3]^T$ and A_p, B_p, and C_p are the system matrices obviously defined. Defining the state feedback gain vector, K_p, as $K_p = [k_1 \ k_2 \ k_3]$ with its elements as $k_1 = \frac{(m_1 + a_{1o})}{b_o}$, $k_2 = \frac{(m_2 + a_{2o})}{b_o}$, and $k_3 = \frac{(m_3 + a_{3o})}{b_o}$, the controller of (24) can be rewritten as

$$u = -K_p\hat{x}_p + K_p R - K_R R - \frac{\hat{x}_4}{b_o} + \frac{1}{b_o}\dot{x}_3^\star \tag{26}$$

where $K_R = [\frac{a_{1o}}{b_o} \ \frac{a_{2o}}{b_o} \ \frac{a_{3o}}{b_o}]$ and $R = [x_1^\star \ x_2^\star \ x_3^\star]^T = [\alpha^\star \ \dot{\alpha}^\star \ \ddot{\alpha}^\star]^T$ is the reference state vector. It is straightforward to show that the dynamics of reference state vector, R, can be written as

$$\dot{R} = A_p R + B_d \dot{x}_3^\star + A_o R \tag{27}$$

where A_o is

$$A_o = \begin{bmatrix} 0 & 0 & 0 \\ 0 & 0 & 0 \\ -a_{1o} & -a_{2o} & -a_{3o} \end{bmatrix}$$

Using (25) to (27) and following some mathematical steps give the tracking error dynamics as

$$\dot{e}_c = (A_p - B_p K_p)e_c - [B_p K_p \ B_d]e_o \tag{28}$$

where $e_c = R - x_p$ is the tracking error and e_o the observer estimation error vector, i.e. $e_o = x - \hat{x}$. Next the observer error dynamics is obtained by subtracting (22) from (21) as

$$\dot{e}_o = (A - LC)e_o + Eh \tag{29}$$

Combining (28) and (29) yields

$$\begin{bmatrix} \dot{e}_c \\ \dot{e}_o \end{bmatrix} = \begin{bmatrix} (A_p - B_p K_p) & -[B_p K_p \ B_d] \\ 0 & (A - LC) \end{bmatrix} \begin{bmatrix} e_c \\ e_o \end{bmatrix} + \begin{bmatrix} 0 \\ E \end{bmatrix} h \tag{30}$$

As the system matrix in (30) is in block-triangular form, it is easy to verify that its eigenvalues are union of the eigenvalues of $(A_p - B_p K_p)$ and $(A - LC)$. Since (A_p, B_p) is controllable and (A, C) observable, stability of the error dynamics of (30) can always

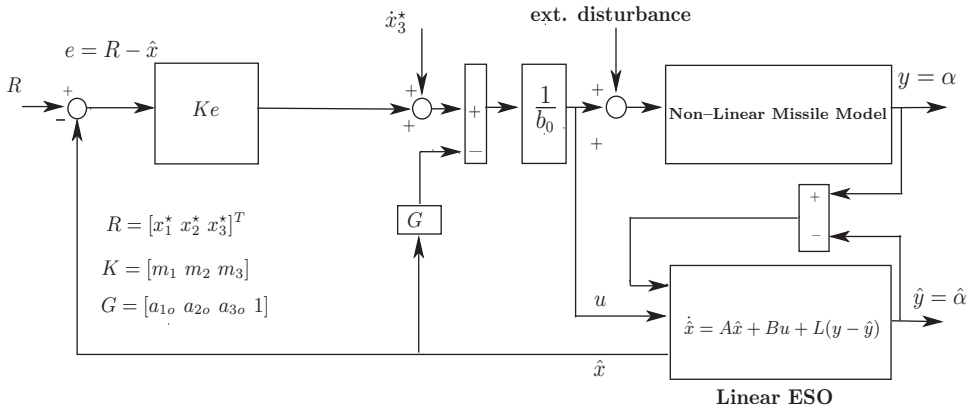

Fig. 1 Functional block diagram of the ESO-based controller

be ensured by placing the controller and observer poles appropriately. Further, since (30) is stable, it is obvious that if h is bounded, bounded input-bounded output stability for the linear dynamics of (30) is assured. When $h=0$, i.e. when the rate of change of uncertainty, d, is zero, the error dynamics of (30) is asymptotically stable and similar result can be expected if the rate of change of the uncertainty is reasonably small.

It may be noted that the quantity h, being the rate of change of the total uncertainty, d, as defined in (16), may be non-linear and state-dependent. As can be seen from (30), h represents a signal which acts as the forcing function or input to the error dynamics and following linear theory, it is obvious that the stability of the error dynamics is governed by the eigenvalues of the system matrix. Thus, while it is necessary that the signal h be bounded, its exact nature or magnitude is not needed for stability analysis. Following similar line, in references [**43**, **44**], the stability issue in the ESO-based control systems has been addressed by considering the quantity h as a bounded function and it is shown that both the state estimation error, e_o, and the closed-loop tracking error, e_c, are bounded and the error upper bounds monotonously decrease with the observer and controller bandwidths. Apart from the ESO-based formulations which appeared in the literature, similar treatment for system uncertainties can be found in other works as well. For example, in reference [**45**], the TDC theory has been extended for designing a robust observer for non-linear plants. The observer error dynamics is driven by system state-dependent non-linearities and uncertainties which are assumed to be bounded and the authors have shown that the resulting steady-state observation error is bounded. Similarly, in reference [**46**], I–O using TDC and time delay observer is proposed. For establishing stability of the overall system, a bounding term on the state-dependent nonlinear term is assumed and using Lyapunov's approach, the authors have shown that the overall error is bounded if the driving term of the error dynamics remains bounded.

As is obvious from (29), the state estimation error dynamics of ESO exhibits asymptotic stability if the rate of change of uncertainties, h, is negligible. Such an assumption may not hold true for systems having either fast varying disturbances/uncertainties or state-dependent uncertainties with fast varying reference signals or both. In such situations, the performance of the ESO presented in section 3.2 may not offer satisfactory results. However, the issue of the fast varying uncertainty too can be dealt within the framework of the ESO by employing a higher order ESO [**47**]. For example, if the rate of change of uncertainty is not negligible, but its second rate is, a second-order ESO can be employed. It can be shown that the estimation error dynamics for the second-order ESO will be asymptotically stable if $\ddot{d}$ is negligible. In fact, it can be shown that an rth order ESO will offer asymptotic stability for the state estimation error dynamics if the rth rate of change of uncertainty is negligible.

5 SIMULATIONS AND RESULTS

Simulations are carried out by applying the ESO-based controller (24) to the missile dynamics (1) to verify the performance of the ESO in estimation of states and uncertainties and its tracking performance. The controller and observer are designed at $M=2.25$ as it represents the midpoint of the considered Mach envelope. The nominal values for the various parameters appearing in the controller (24) are taken from Table 1. The controller gains, m_i's required in (24) are obtained by placing the closed-loop poles at $(1+\frac{\tau_c}{3}s)^3$ with a time constant $\tau_c=0.25$. Similarly, the ESO linear gains β_i's are obtained by placing the observer poles at $(1+\frac{\tau_o}{4}s)^4$ with $\tau_o=\tau_c/60$. The observer time constant is chosen by observing the simulated responses. The initial conditions for the observer as well as for the plant are taken as zero. The missile dynamics is simulated for a series of commanded manoeuvres which exercise the control characteristics of this design. To this end, the reference angle of attack profile is taken as $\alpha^*=15^\circ$ for $0<t\leqslant 2$ s, $\alpha^*=-8^\circ$ for $2<t\leqslant 4$ s, and $\alpha^*=10^\circ$ for $t>4$ s. As the reference angle of attack changes in step, the rate of change of it and its higher derivatives are taken as zero. For the purpose of comparison of actual uncertainty with its estimated value, actual uncertainty is computed from (17) as $d=\ddot{\alpha}-a_{1o}\alpha-a_{2o}\dot{\alpha}-a_{3o}\ddot{\alpha}-b_o u$, where the a_{io} and b_o are computed using the nominal values of the parameters. Also, to smoothen the reference, the commanded signal is passed through a first-order filter of time constant of 0.01 [**5**, **9**, **17**]. With these data, first simulations are carried out for $M=2.25$ and the results presented in Fig. 2. From Fig. 2 (a), it may be observed that the output has tracked the reference quite accurately. In Figs 2(a) to (c), estimated states are plotted along with the actual ones and it can be seen that the ESO has achieved accurate state estimation. The time histories of the actual and estimated uncertainties are given in Fig. 2(d) from where it can be observed that the ESO has estimated the uncertainty quite satisfactorily. The control input history is shown in Fig. 2(e).

Next simulations are carried out by including the variation in Mach number using (2) with $M(0)=3$.

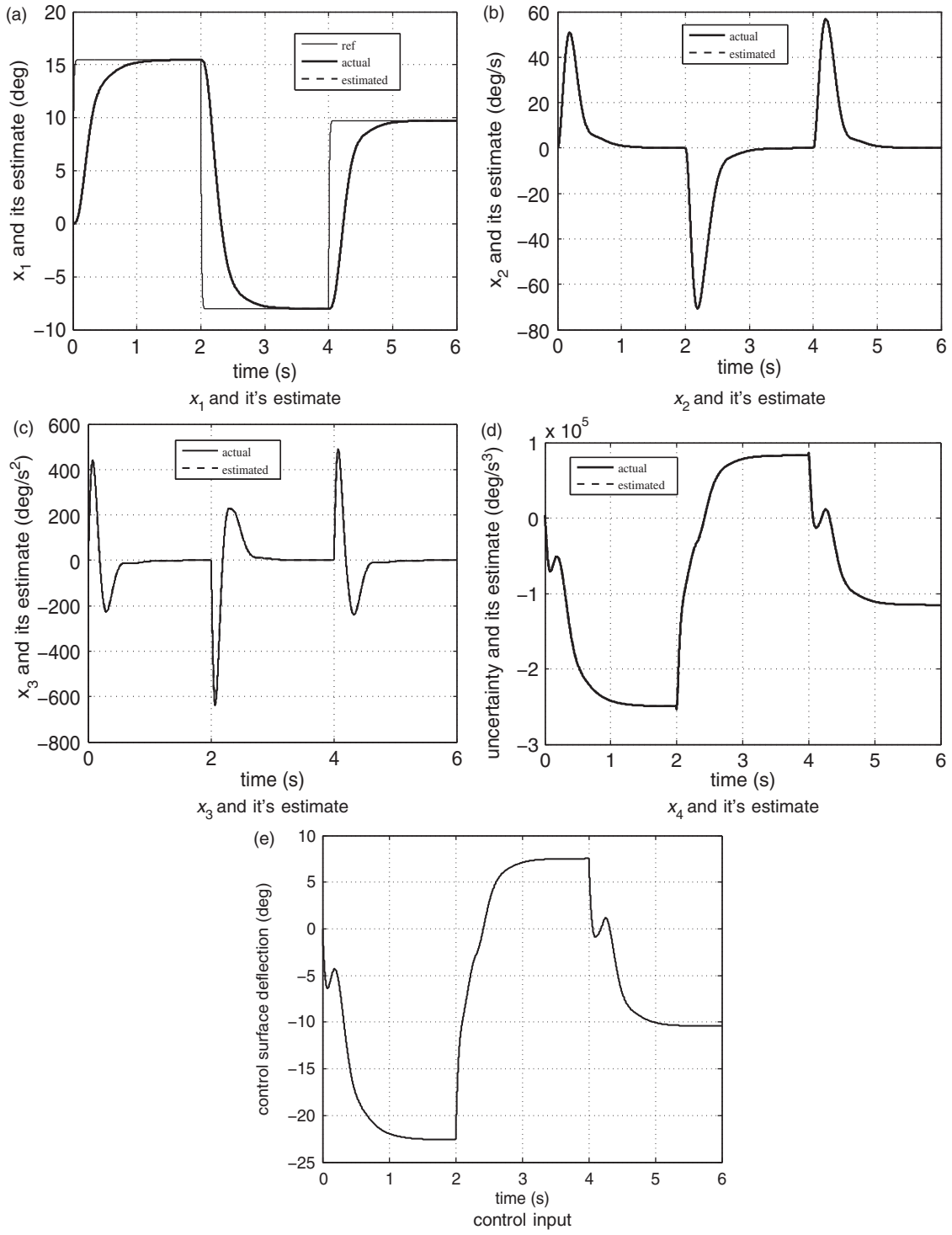

Fig. 2 Performance of ESO in state estimation

The normal and longitudinal accelerations needed in (2) are taken as [**3**]

$$a_z = K_z M^2(t) C_n[\alpha(t), \delta(t), M(t)]$$

$$a_x = \frac{0.7 P_0 S C_a}{m}$$

In simulation, the controller employed the same nominal values corresponding to $M = 2.25$, thus introducing significant uncertainty in the plant owing to variation in Mach number. The results are as shown in Fig. 3. From Fig. 3(a), it can be observed that the controller achieved accurate tracking of

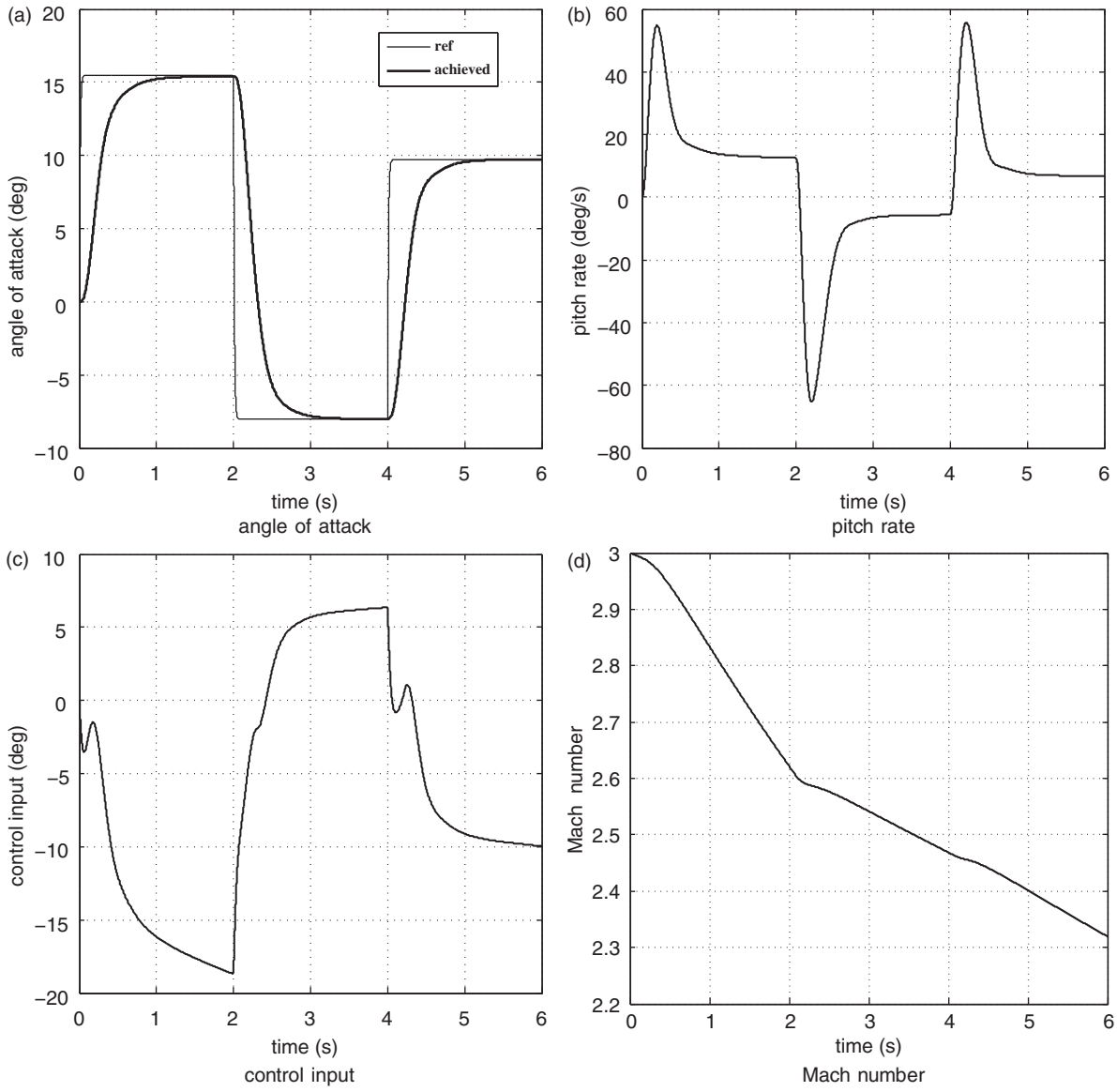

Fig. 3 Performance of ESO-based controller with Mach dynamics

commanded angle of attack in spite of the uncertainty introduced in the missile dynamics due to Mach number variation. Figures 3(b) to (d) gives the corresponding pitch rate, control input, and Mach number histories, respectively. Next, simulations are carried out by introducing uncertainty, un-modelled dynamics, and control input, as well as rate saturation and the results are presented along with the results of some of the well-known existing controllers in the next section.

6 COMPARISON WITH EXISTING DESIGNS

This section presents results on performance comparison of the proposed design with some well-known designs existing in the literature. The designs considered are: (1) IOL controller, (2) predictive controller (PC), (3) SMC-based design, and (4) the proposed ESO-based design. For the sake of a valid comparison, all the controllers are designed at $M = 2.25$ and for the controller time constant of 0.25 s, significant uncertainties are introduced in C_n and C_m in the plant (1). First, a brief note of each of the controller considered for comparison is presented.

6.1 IOL controller (IOL)

The IOL control law considered is the same as given by (18) and reproduced here for the sake of reference

$$u = \frac{1}{b_o}\Big[- a_{1o}\alpha - a_{2o}\dot{\alpha} - a_{3o}\ddot{\alpha} - d + \dddot{\alpha}^{\star} + m_1(\alpha^{\star} - \alpha) + m_2(\dot{\alpha}^{\star} - \dot{\alpha}) + m_3(\ddot{\alpha}^{\star} - \ddot{\alpha})\Big] \tag{31}$$

In the controller design, the contribution of δ in force equation is ignored and also $cos(\alpha)$ is approximated to 1. The values of the controller gains m_1, m_2, and m_3 are the same as those of the ESO-based controller. The control law needs $\dot{\alpha}$ and $\ddot{\alpha}$ and the same are obtained by numerical differentiation of the plant output, α, in simulations of this controller. Finally, the uncertainty, d, required in this controller is obtained analytically as

$$d = K_q M^2(3a_m k^3\alpha^2 + 2b_m k^2|\alpha|)\dot{\alpha} - K_q M^2 d_m k\omega_a\delta + K_\alpha M(6a_n k^3\alpha + 2b_n k^2 sign(\alpha))\dot{\alpha}^2 + K_\alpha M(3a_n k^3\alpha^2 + 2b_n k^2|\alpha|)\ddot{\alpha}$$

6.2 Predictive controller (PC)

The next controller considered for comparison purpose is based on the non-linear continuous time predictive control technique. In this approach [**48**], the future response of the states or output of a non-linear dynamic system is predicted by appropriate functional expansion, and a quadratic cost function based on the errors between the predicted and the desired responses and the current control expenditure is minimized point-wise to obtain a continuous time-optimal, non-linear feedback control law. A design of an angle of attack tracking controller based on this approach is presented in reference

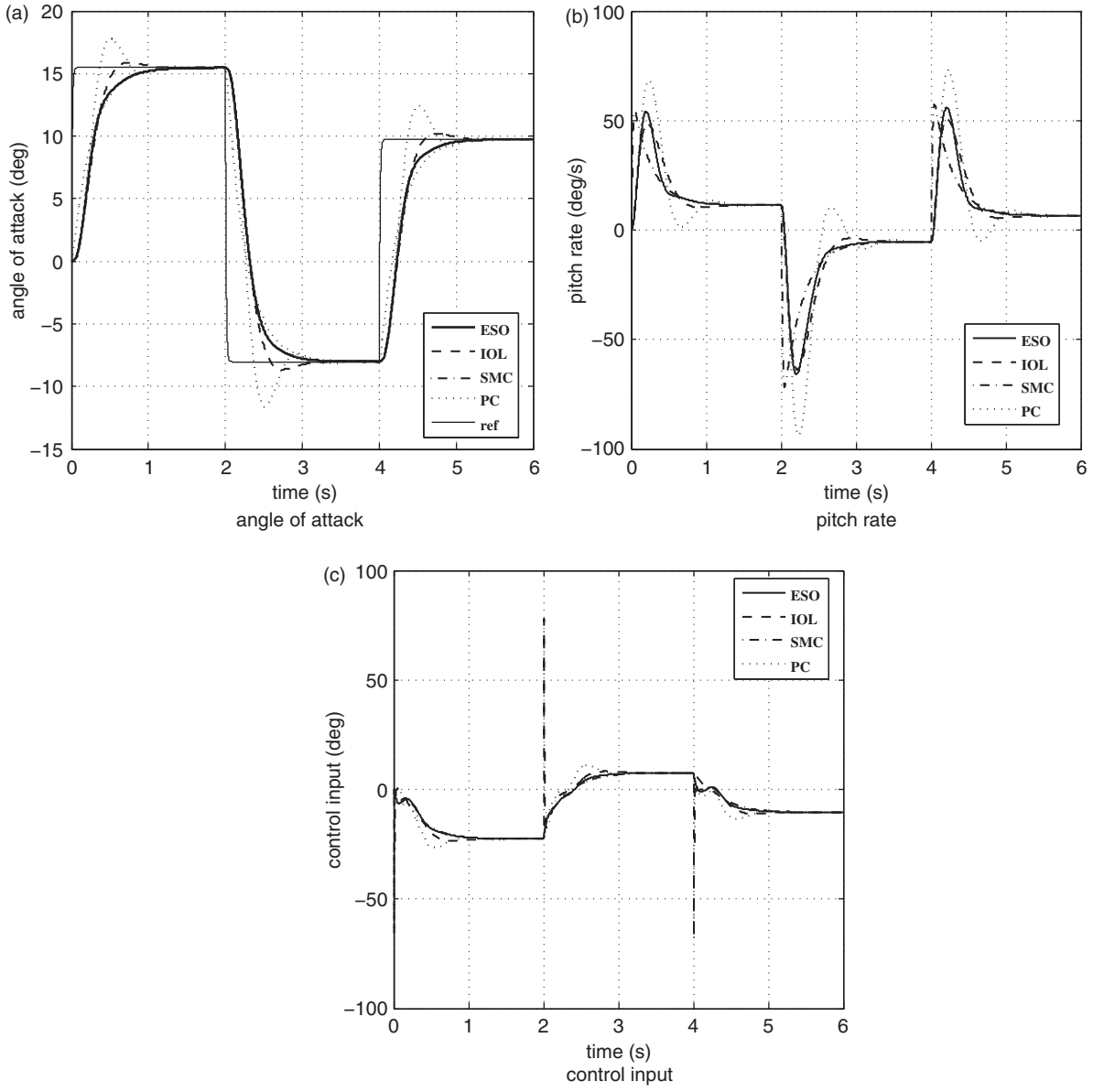

Fig. 4 Performance of ESO-based controller without uncertainty

[**10**], and the same is used here. The control law is given by

$$u = -\frac{6}{b_p \Delta t^3}\left[e + \Delta t\dot{e} + \frac{\Delta t^2}{2}\ddot{e} + \frac{\Delta t^3}{6}(a_p - \ddot{\alpha}^\star)\right] \tag{32}$$

where Δt represents the predictive horizon, e, the output tracking error, i.e. $e = \alpha - \alpha^*$, and the functions a_p and b_p are given as

$$\begin{aligned} a_p &= K_q M^2(3a_m k^3\alpha^2 + 2b_m k^2|\alpha| + c_m(-7+8M/3)k)\dot{\alpha} \\ &\quad - K_q M^2 d_m k w_a \delta + K_\alpha M(6a_n k^3\alpha + 2b_n k^2 sign(\alpha))\dot{\alpha}^2 \\ &\quad + K_\alpha M(3a_n k^3\alpha^2 + 2b_n k^2|\alpha| + c_n(2-M/3)k)\ddot{\alpha} \\ b_p &= K_q M^2 d_m k w_a \end{aligned}$$

In simulations, the value of prediction horizon, $\Delta t = 0.18$ is used.

6.3 Sliding-mode control (SMC)

SMC is a robust method for the control of systems with significant uncertainties and unmeasurable disturbances. In this approach, insensitivity to uncertainties is achieved by employing a discontinuous control based on the bound of uncertainties. However, in reality, the exact value of the bound is rarely known. If the uncertainty is smaller than the assumed bound, the performance is satisfactory; however, the resulting control is large. On the other hand, if the bound is smaller than the uncertainty, the response may not be satisfactory. In addition, the

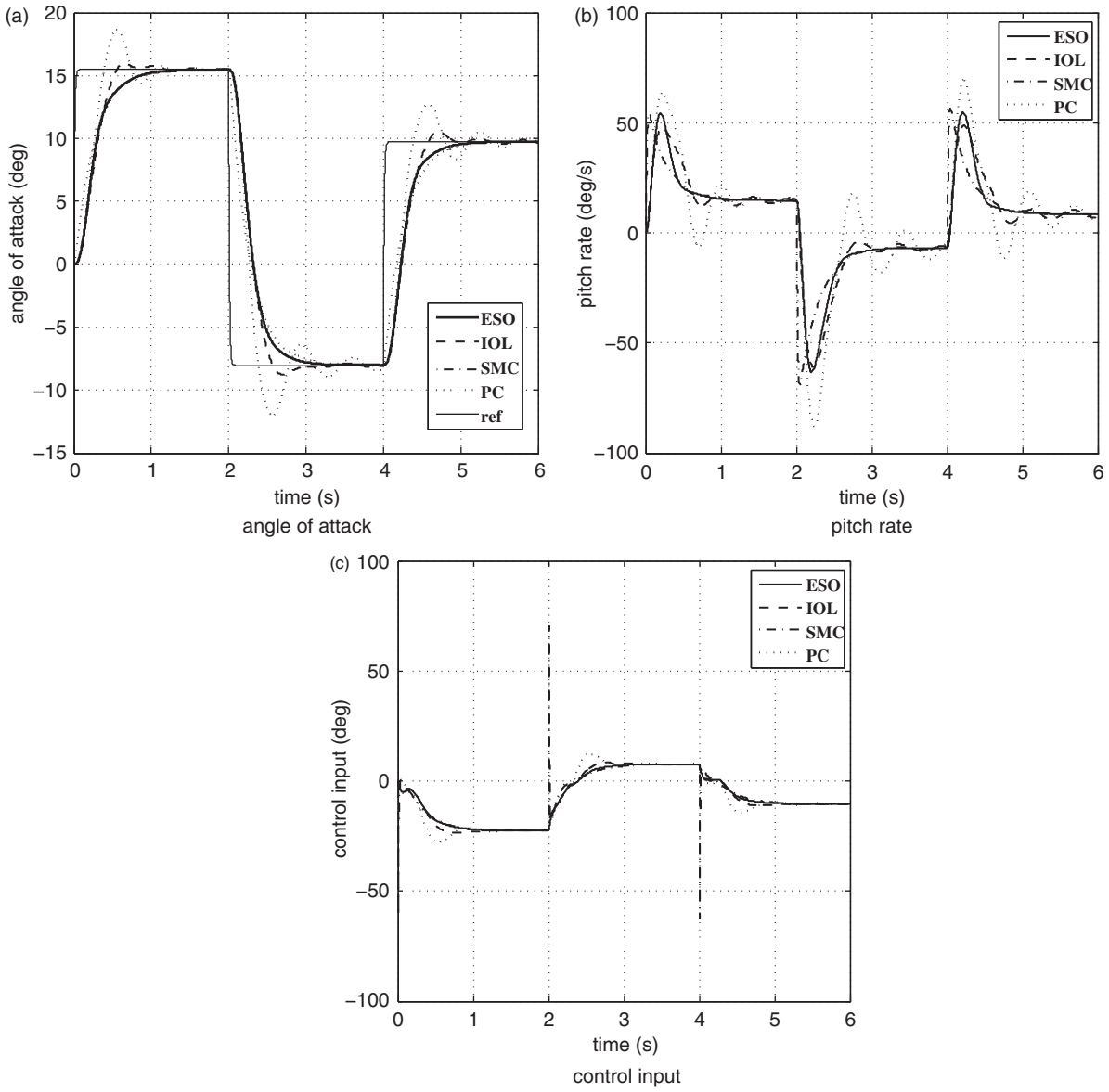

Fig. 5 Performance of ESO-based controller with +30 per cent uncertainty in C_n and C_m

controller needs plant states for its implementation. In this study, the control law and design parameters as given in reference [**49**] are used. The control law is given by

$$u = \frac{1}{b_s}(-\nu(x,t) - \rho \text{sgn}(s)) \tag{33}$$

where s is the switching surface given by $s(t) = \dot{e}(t) + \lambda e(t)$ and $e(t) = \alpha - \alpha^*$. The quantity, sgn(s), is the signum function defined as

$$\text{sgn}(s) = \begin{cases} 1 & \text{if } s > 0 \\ 0 & \text{if } s = 0 \\ -1 & \text{if } s < 0 \end{cases}$$

The discontinuity in the control law is dealt with by defining a boundary layer of width ϕ around the sliding surface, i.e. replacing sgn(s) with a continuous saturation function sat(s/ϕ), where sat(x) = x if $|x| \leqslant 1$ and sat(x) = sgn(x) otherwise. The quantities b_s and ν are given as

$$b_s = K_\alpha M d_n k \omega_a$$

$$\begin{aligned}\nu(x,t) = {} & \lambda \dot{e} - \ddot{\alpha}_d + K_\alpha M[(3a_n k^3 \alpha^2 + 2b_n k^2 |\alpha| \\ & + c_n(2 - M/3)k)\dot{\alpha}\cos(\alpha) - C_n \sin(\alpha)\dot{\alpha}] \\ & - K_\alpha M d_n k \omega_a \delta + \dot{q}\end{aligned}$$

In simulations, the controller design parameters considered are $\lambda = 4$, $\rho = 80$, and $\phi = 0.5$.

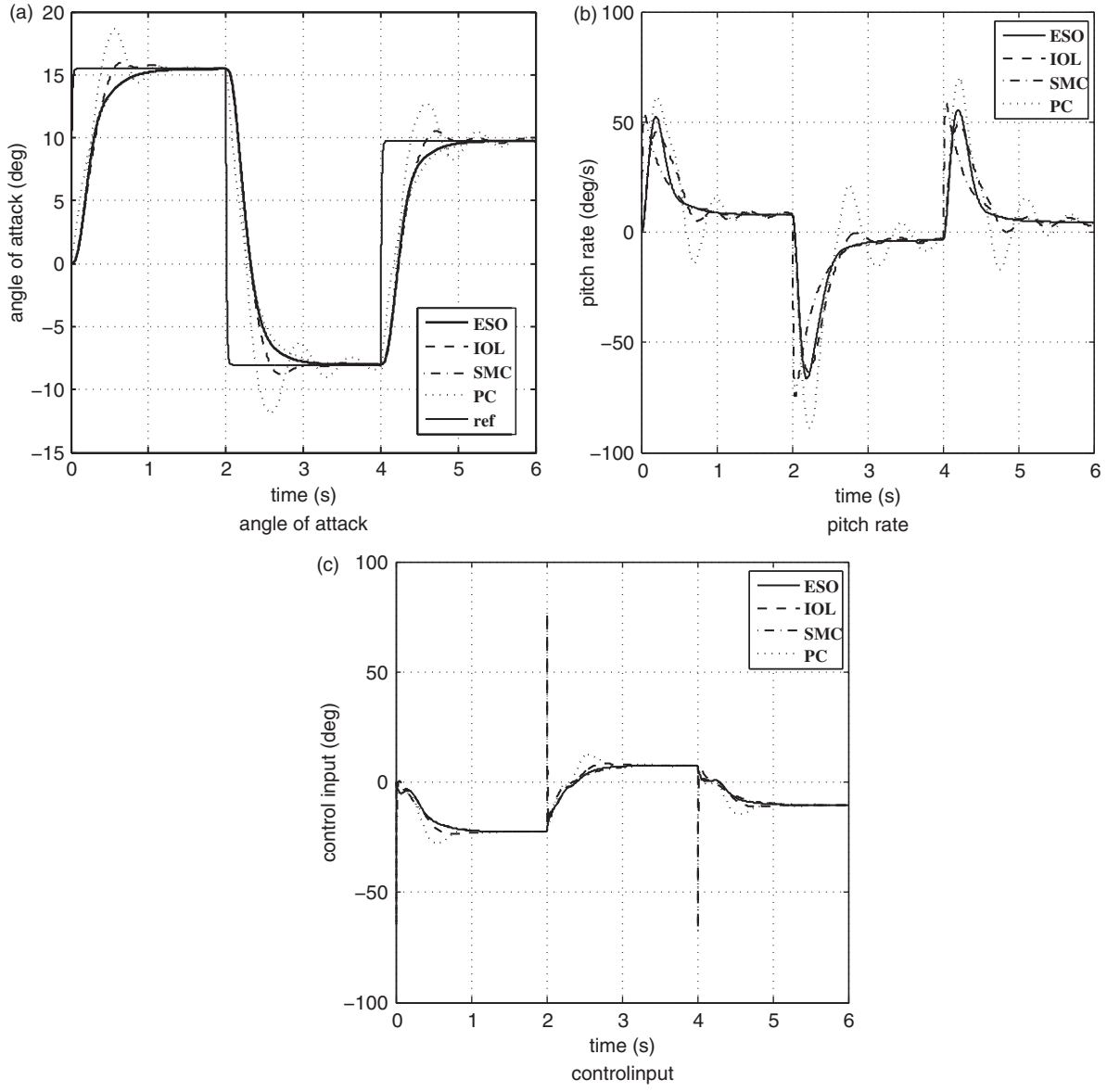

Fig. 6 Performance of ESO-based controller with +30 per cent uncertainty in C_m and −30 per cent uncertainty in C_n

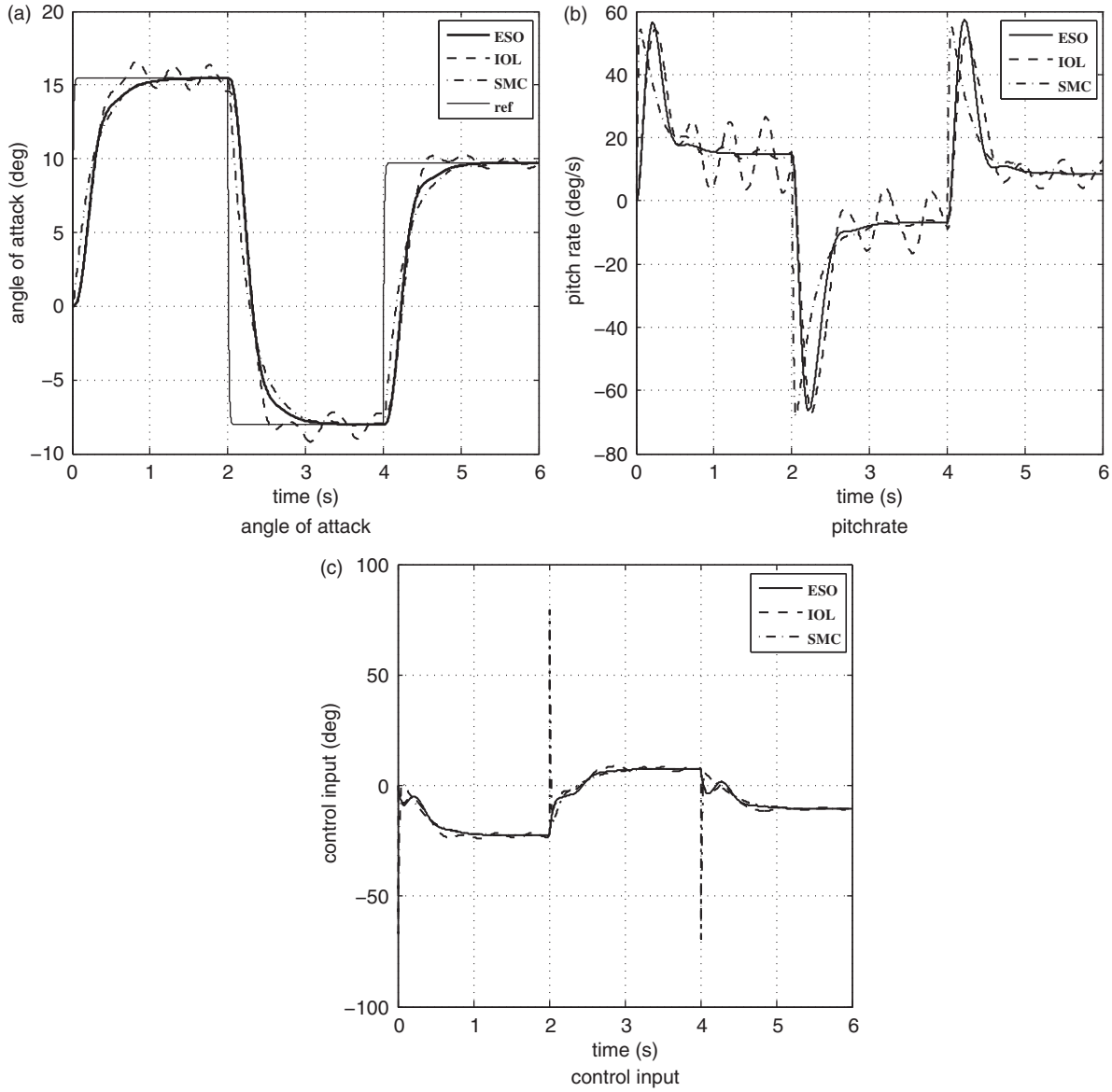

Fig. 7 Performance of ESO-based controller with −30 per cent uncertainty in C_m and +30 per cent uncertainty in C_n

6.4 ESO-based control

The proposed control law given by (24) represents the ESO-based control in the comparison study.

6.5 Performance comparison

First simulations are carried out without considering uncertainty in C_n and C_m and the results are as shown in Fig. 4. From Fig. 4(a), it may be observed that while the performances of the SMC and ESO-based controllers are quite similar, the predictive control exhibits higher overshoot followed by the IOL control. Next, simulations are carried out by considering ± 30 per cent uncertainties in C_n and C_m and the results are presented in Figs 5 to 8. During simulations, it is observed that the PC goes unstable for the cases when $C_m = -30$ per cent, $C_n = 30$ per cent $C_m = -30$ per cent, $C_n = -30$ per cent and hence its results are omitted in the respective figures. From the figures, it can be observed that in all the cases of uncertainties, the performance of the proposed ESO-based controller is uniformly satisfactory. It can also be noted that the predictive as well as the IOL control exhibit overshoots in the angle of attack response. Finally, while the SMC tracking performance is quite close to the ESO-based control, the control exhibits discontinuity in control action at 2 and 4 s.

Next, a more realistic scenario is considered to check the performances of the controllers. A wind

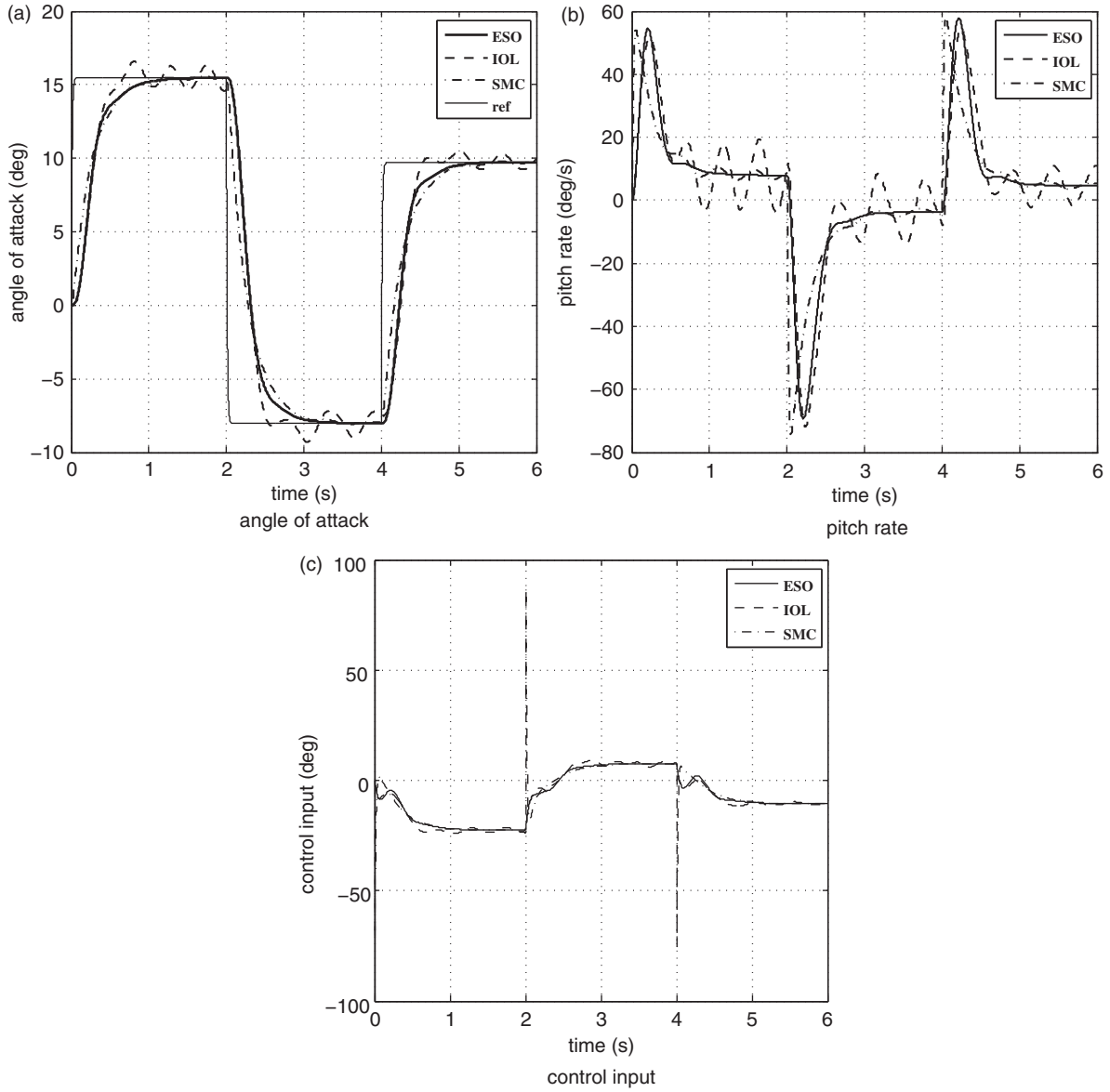

Fig. 8 Performance of ESO-based controller with −30 per cent uncertainty in C_m and −30 per cent uncertainty in C_n

gust, modelled as a sinusoidal disturbance of magnitude 8° and frequency 0.25 Hz is introduced as an external disturbance in the input channel. Further, a time delay of 0.1 s is introduced which may represent the delays involved in the control loop as well as the effect of un-modelled dynamics. Parametric uncertainty of +20 per cent in C_m and −20 per cent in C_n is also introduced and the results are presented in Fig. 9. From the figures, it can be observed that all the controllers, except the proposed ESO-based control, result in highly oscillatory responses.

Finally, simulations are carried out by considering control input and rate saturations. As it is well known, in practice, physical limitations will always exist on actuator deflection and its rate. The missile may be commanded to follow a highly varying α profile; however, due to these constraints, the response of the missile may get adversely affected. To this end, limits are imposed on control input and its rate by considering $-30^\circ \leqslant \delta \leqslant 30^\circ$ and $\dot{\delta}$ is constrained to 25 deg/s/g acceleration command. Simulations are carried out using the stated constraints and without any uncertainty for all the controllers. During simulations, it is observed that while the predictive control and SMC resulted in instability, the IOL control resulted in poor tracking and in view of this, the results for ESO-based design alone are presented. For the sake of comparison, simulations are performed with and without the constraints and the results are presented with the suffix sat and nom for

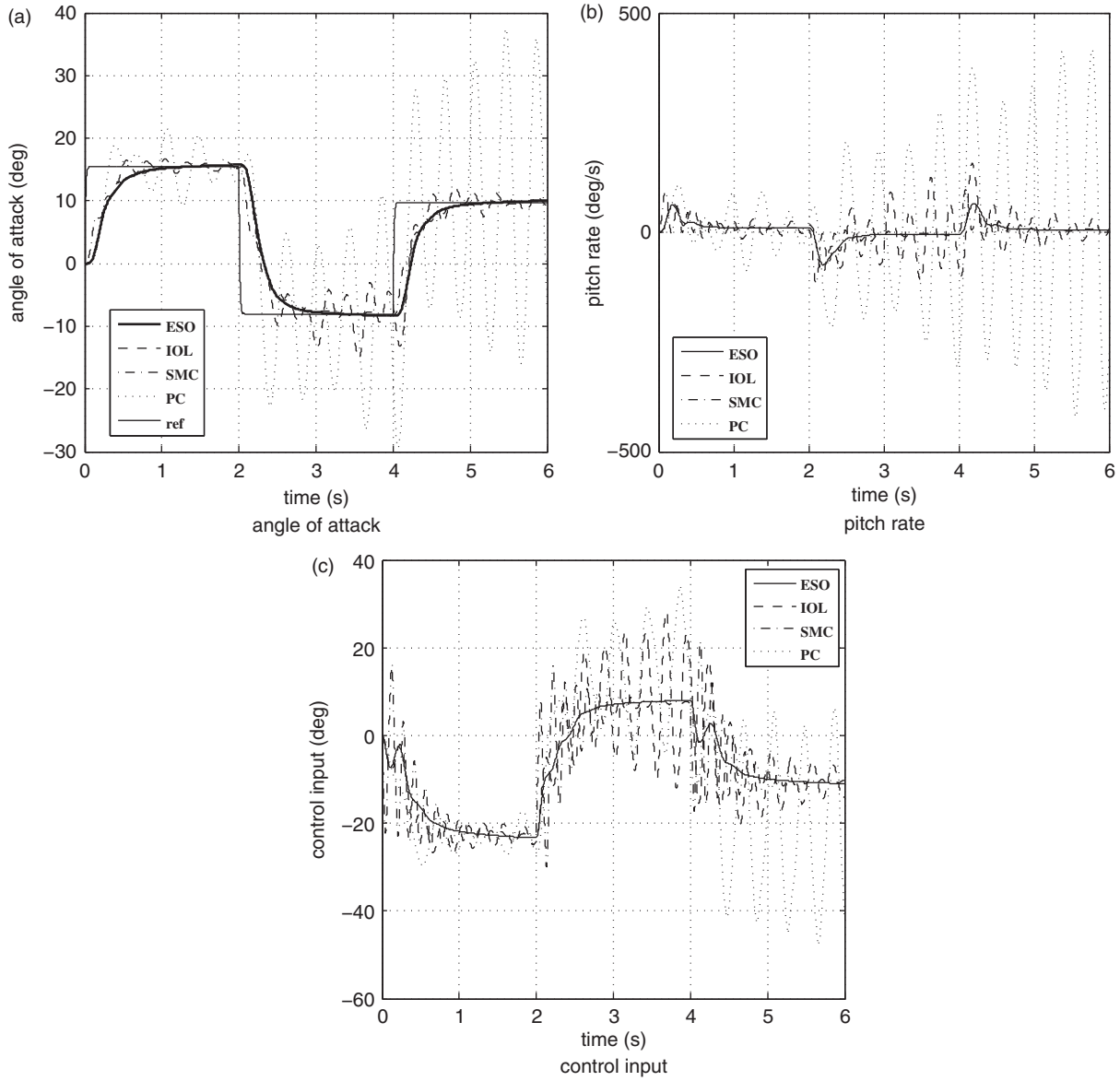

Fig. 9 Performance of ESO-based controller with +20 per cent uncertainty in C_m and −20 per cent uncertainty in C_n, wind gust and time delay

these cases, respectively. The results are shown in Fig. 10 and it can be observed that the proposed ESO-based design has offered quite satisfactory tracking performance notwithstanding the considered hard constraints.

In the simulation results presented in this section, it is important to note that the IOL, predictive, and SMC controllers have been implemented using exact values of the states. It is logical that when the controllers are implemented in conjunction with a separately designed observer, the performance would not be the same. On the other hand, the ESO-based controller used the ESO estimated states. In general, the proposed ESO-based design offers certain distinct advantages. First, it does not require any knowledge, such as bound, of uncertainty nor exact system model and is robust. Second, the controller does not need availability of all the states as the ESO estimates the states as well as the uncertainty in an integrated manner. Third, the controller is computationally efficient compared to many other formulations presented in the literature. Finally, as seen from the results in Fig. 3, a single design works for the complete flight envelope. In view of this, it is hoped that it has potential to address the issues and complexities associated with the gain scheduling approach.

7 CONCLUSIONS

In this article, a robust pitch autopilot design based on the ESO is proposed for a cruciform, roll-position

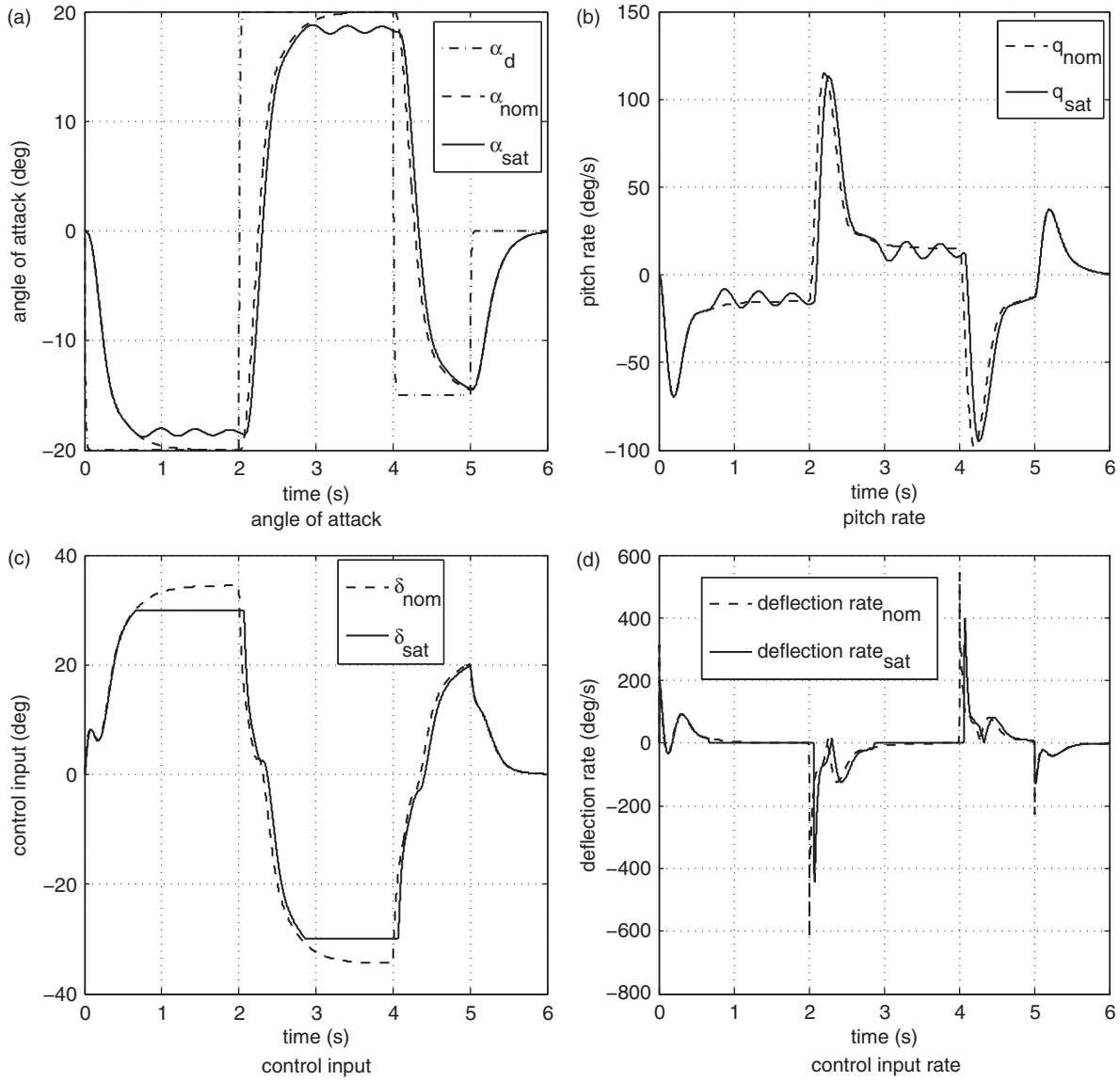

Fig. 10 Performance of ESO-based controller with input and rate saturation

stabilized, tail-controlled missile. The ESO treats the effects of system uncertainty, external disturbance, and modelling inaccuracies together as a lumped entity and estimates it along with the system state in an integrated manner. The ESO is integrated with the IOL controller designed for the nominal model to achieve robustness. The effectiveness of the ESO in estimation of the states and uncertainty and the efficacy of the ESO-based controller in tracking the commanded angle of attack in the presence of significant uncertainties are demonstrated through simulation. The results show that the controller offers satisfactory tracking of the desired command in spite of considerable uncertainties, un-modelled dynamics, and non-linearities. A comparison of the proposed design with the various other methods in the literature clearly brings out the superiority of the proposed design in terms of robustness as well as performance.

FUNDING

This research received no specific grant from any funding agency in the public, commercial, or not-for-profit sectors.

ACKNOWLEDGEMENT

The first author would like to acknowledge the authorities of Bharati Vidyapeeth University College of Engineering, Pune-411 043, India for their support during the course of this work.

REFERENCES

1 **Garnell, P.** *Guided weapon control systems*, edition 2, 1980 (Pergamon Press, Oxford, UK).
2 **Horton, M. P.** Autopilots for tactical missiles: an overview. *Proc. IMechE, Part I: J. Systems and Control Engineering*, 1995, **209**, 127–139.
3 **Nichols, R. A., Reichert, R. T.,** and **Rugh, W. J.** Gain scheduling for H-infinity controllers: A flight control example. *IEEE Trans. Control Syst. Technol.*, 1993, **1**(2), 69–78.
4 **Reichert, R. T.** Dynamic scheduling of modern robust control autopilot designs for missiles. *IEEE Control Syst. Mag.*, 1992, **12**(5), 35–42.
5 **Theodoulis, S.** and **Duc, G.** Missile autopilot design: gain scheduling and the gap metric. *J. Guid. Control Dyn.*, 2009, **32**(3), 986–996.
6 **Bennani, S., Willemsen, D. M. C.,** and **Scherer, C. W.** Robust control of linear parametrically varying systems with bounded rates. *J. Guid. Control Dyn.*, 1998, **21**(6), 916–922.
7 **Shamma, J. S.** and **Cloutier, J. R.** Gain-scheduled missile autopilot design using linear parameter varying transformations. *J. Guid. Control Dyn.*, 1993, **16**(2), 256–269.
8 **Mehrabian, A. R.** and **Roshanian, J.** Skid-to-turn missile autopilot design using scheduled eigenstructure assignment technique. *Proc. IMechE, Part G: J. Aerospace Engineering*, 2006, **220**, 225–239.
9 **Zhu, J. J.** and **Mickle, M. C.** Missile autopilot design using a new linear time-varying control technique. *J. Guid. Control Dyn.*, 1997, **20**(1), 150–157.
10 **Upreti, V., Talole, S. E.,** and **Phadke, S. B.** Predictive estimation and control based missile autopilot design. In: Proceedings of the AIAA Guidance, Navigation, and Control Conference and Exhibit, Providence, Rhode Island, USA, 16–19 August 2004. Paper no. AIAA 2004–5331.
11 **Choe, D.-G.** and **Kim, J.-H.** Pitch autopilot design using model-following adaptive sliding mode control. *J. Guid. Control Dyn.*, 2004, **25**(4), 826–829.
12 **Kim, S.-H., Kim, Y.-S.,** and **Song, C.** A robust adaptive nonlinear control approach to missile autopilot. *Control Eng. Pract.*, 2003, **12**, 149–154.
13 **Slotine, J.-J. E.** and **Li, W.** *Applied nonlinear control*, 1991 (Prentice-Hall, Englewood Cliffs, New Jersey).
14 **Vidyasagar, M.** *Nonlinear systems analysis*, 1993 (Prentice-Hall, Englewood Cliffs, New Jersey).
15 **Hull, R. A., Schumacher, D.,** and **Qu, Z.** Design and evaluation of robust nonlinear missile autopilots from a performance perspective. In Proceedings of the American Control Conference, Washington, Seattle, June 1995, pp. 189–193.
16 **Chen, W.-H.** Nonlinear disturbance observer-enhanced dynamic inversion control of missile. *J. Guid. Control Dyn.*, 2003, **26**(1), 161–166.
17 **Calise, A. J., Sharma, M.,** and **Corban, J. E.** Adaptive autopilot design for guided munitions. *J. Guid. Control Dyn.*, 2000, **23**(5), 837–843.
18 **Bruyere, L., Tsourdos, A.,** and **White, B. A.** Robust augmented lateral acceleration flight control design for a quasi-linear parameter-varying missile. *Proc. IMechE, Part G: J. Aerospace Engineering*, 2005, **219**, 171–181.
19 **Tsourdos, A., Blumel, A. L.,** and **White, B. A.** Flight control design for a missile-an approximate feedback linearization approach. In Proceedings of the 7th Mediterranean Conference on *Control and automation* (MED99), Haifa, Israel, 28–30 June 1999, pp. 593–602.
20 **Tsourdos, A.** and **White, B. A.** Adaptive flight control design for nonlinear missile. *Control Eng. Pract.*, 2005, **13**(3), 373–382.
21 **Lin, C. C.** and **Chen, F. C.** Improving conventional longitudinal missile autopilot using cerebellar model articulation controller neural networks. *J. Guid. Control Dyn.*, 2003, **26**(5), 711–718.
22 **Chen, J. S.** and **Chen, Y. H.** Robust control of nonlinear uncertain system: A feedback linearization approach. In Proceedings of the 30th IEEE Conference on *Decision and control*, Brighton, England, 1–3 December 1991, pp. 2515–2519.
23 **Huang, J., Lin, C. F., Cloutier, J. R., Evers, J. H.,** and **D'Souza, C.** Robust feedback linearization approach to autopilot design. In Proceedings of the IEEE Conference on *Control applications*, Dayton, Ohio, USA, 13–16 September 1992, pp. 220–225.
24 **Slotine, J.-J. E.** and **Hedrick, J. K.** Robust input-output feedback linearization. *Int. J. Control*, 1993, **57**(5), 1133–1139.
25 **Fernandez, R. B.** Robust feedback linearization through sliding mode control. In Proceedings of the 29th IEEE Conference on *Decision and control*, Honolulu, Hawaii, USA, 5–7 December 1990, pp. 3398–3399.
26 **Talole, S. E., Godbole, A. A., Kolhe, J. P.,** and **Phadke, S. B.** Robust roll autopilot design for tactical missiles. *J. Guid. Control Dyn.*, 2011, **34**(1), 107–117.
27 **Talole, S. E., Ghosh, A.,** and **Phadke, S. B.** Proportional navigation guidance using predictive and time delay control. *Control Eng. Prac.*, 2006, **14**(12), 1445–1453.
28 **Talole, S. E.** and **Phadke, S. B.** Robust input-output linearisation using uncertainty and disturbance estimation. *Int. J. Control*, 2009, **82**(10), 1794–1803.
29 **Hall, C. E.** and **Shtessel, Y. B.** Sliding mode disturbance observer-based control for a reusable launch vehicle. *J. Guid. Control Dyn.*, 2006, **29**(6), 1315–1328.
30 **Williams, D. E., Friedland, B.,** and **Madiwale, A. N.** Modern control theory for design of autopilots for bank-to-turn missiles. *J. Guid. Control Dyn.*, 1987, **10**(4), 378–386.
31 **Wang, W.** and **Gao, Z.** A comparison study of advanced state observer design techniques. In Proceedings of the American Control Conference. Denver, Colarado, USA, June 2003, pp. 4754–4759.
32 **Gao, Z., Huang, Y.,** and **Han, J.** An alternative paradigm for control system design. Proceedings of the 40th IEEE Conference on *Decision and control*, Orlando, Florida, USA, 4–7 December 2001, pp. 4578–4585.
33 **Yoo, D., Yau, S. S.-T.,** and **Gao, Z.** Optimal fast tracking observer bandwidth of the linear extended state observer. *Int. J. Control*, 2007, **80**(1), 102–111.

34 Xia, Y., Shi, P., Liu, G. P., Rees, D., and **Han, J.** Active disturbance rejection control for uncertain multivariable systems with time delay. *IET Control Theory Appl.*, 2007, **1**(1), 75–81.

35 Talole, S. E., Kolhe, J. P., and **Phadke, S. B.** Extended-state-observer-based control of flexible-joint system with experimental validation. *IEEE Trans. Ind. Electro.*, 2010, **57**(4), 1411–1419.

36 Huang, Y., Xu, K., Han, J., and **Lam, J.** Flight control design using extended state observer and non-smooth feedback. In Proceedings of the 40th IEEE Conference on *Decision and control*, Orlando, Florida, USA, 4–7 December 2001, pp. 223–228.

37 Xia, Y., Zhu, Z., Fu, M., and **Wang, S.** Attitude tracking of rigid spacecraft with bounded disturbances. *IEEE Trans. Ind. Electro.*, 2011, **58**(2), 647–659.

38 Zhang, R. and **Tong, C.** Torsional vibration control of the main drive system of a rolling mill based on an extended state observer and linear quadratic control. *J. Vib. Control*, 2006, **12**(3), 313–327.

39 Feng, G., Liu, Y.-F., and **Huang, L.** A new robust algorithm to improve the dynamic performance on the speed control of induction motor drive. *IEEE Trans. Ind. Electro.*, 2004, **19**(6), 1614–1627.

40 Su, Y. X., Zheng, C. H., and **Duan, B. Y.** Automatic disturbances rejection controller for precise motion control of permanent-magnet synchronous motors. *IEEE Trans. Ind. Electro.*, 2005, **52**(3), 814–823.

41 Su, J., Qiu, W., Ma, H., and **Woo, P.-Y.** Calibration-free robotic eye-hand coordination based on an auto disturbance rejection controller. *IEEE Trans. Rob.*, 2004, **20**(5), 899–907.

42 Su, J., Ma, H., Qiu, W., and **Xi, Y.** Task-independent robotic uncalibrated hand-eye coordination based on the extended state observer. *IEEE Trans. Syst. Man. Cybernet.*, 2004, **34**(4), 1917–1922.

43 Zheng, Q., Dong, L., Lee, D. H., and **Gao, Z.** Active disturbance rejection control for MEMS gyroscopes. *IEEE Trans. Control Syst. Technol.*, 2009, **17**(6), 1432–1438.

44 Zheng, Q., Chen, Z., and **Gao, Z.** A practical approach to disturbance decoupling control. *Control Eng. Pract.*, 2009, **17**, 1016–1025.

45 Chang, P. H., Lee, J. W., and **Park, S. H.** Time delay observer: a robust observer for nonlinear plants. *Trans. ASME, J. Dyn. Sys. Meas. Control*, 1997, **119**, 521–527.

46 Lee, J. W. and **Chang, P. H.** Input/output linearisation using time delay control and time delay observer. In Proceedings of the American Control Conference, Philadelphia, Pennsylvania, USA, 24–26 June 1998, pp. 318–322.

47 Miklosovic, R., Radke, A., and **Gao, Z.** Discrete implementation and generalization of the extended state observer. Proceedings of the American Control Conference, Minneapolis, Minnesota, USA, 14–16 June 2006, pp. 2209–2214.

48 Lu, P. Nonlinear predictive controllers for continuous systems. *J. Guid. Control Dyn.*, 1994, **17**(3), 553–560.

49 Bahrami, M., Ebrahimi, B., Ansarifar, G. R., and **Roshanian, J.** Sliding mode autopilot and observer design for a supersonic flight vehicle. In Proceedings of the 2nd International Symposium on *Systems and control in aerospace and astronautics*, 10–12 December, 2008, pp. 1–5 (Shenzhen).

APPENDIX

Notation

a_m, b_m, c_m	polynomial coefficients of angle of attack component of aerodynamic moment coefficient
a_n, b_n, c_n	polynomial coefficients of angle of attack component of aerodynamic force coefficient
a_z, a_x	normal and longitudinal accelerations, respectively, of missile (m/s^2)
a_{1o}, a_{2o}, a_{30}	nominal values of the respective coefficients
a_1, a_2, a_3	coefficients in $\ddot{\alpha}$ equation
A	system matrix
A_p	plant system matrix
b	actual value of control input gain
b_o	nominal value of control input gain
B	input matrix
B_d	disturbance input matrix
B_p	input matrix of plant
C	output matrix
C_a	drag coefficient
C_m	pitch moment coefficient
C_n	normal force coefficient
d_r	diameter (m)
d	total uncertainty
$\acute{d}$	non-linear terms in $\ddot{\alpha}$ equation
d_m	tail fin deflection component of aerodynamic moment coefficient
d_n	tail fin deflection component of aerodynamic force coefficient
e_c	closed-loop state tracking error vector
e_o	state estimation error vector
E	observer error dynamics disturbance input matrix
h	rate of change of uncertainty
k	radian-to-degree conversion factor
I_y	pitch moment of inertia (kg/m^2)
K_p	state feedback gain vector
K_α, K_q, K_z	missile flight parameters
L	ESO gain vector
m	mass of missile (kg)
m_i	gains in output tracking error dynamics
M	Mach number
P_0	static pressure (N/m^2)
q	pitch rate (rad/s)
R	reference state trajectory vector
S	surface area (m^2)

v_s	speed of sound (m/s)
w	external disturbance
x	extended system state vector
$\hat{x}$	observer estimated state vector
x_p	plant state vector
y	system output
$\hat{y}$	observer output
α	angle of attack (rad)
β_i	elements of ESO gain vector
δ	actual tail fin deflection (rad)
δ_c	commanded tail fin deflection (rad)
Δa_{io}	uncertainty associated with a_i
Δb	uncertainty associated with b
ω_a	actuator bandwidth (rad/s)
ζ_a	actuator damping
ϵ	a positive number to limit gain in neighbourhood of origin in ESO
τ_c	controller time constant
τ_o	observer time constant
λ	positive constant defining the bandwidth of the error dynamics
ρ	positive constant that determines the desired reaching time to the sliding surface
ϕ	width of boundary layer